Biointerface Research in Applied Chemistry
Open-Access Journal (ISSN: 2069-5837)

Article
Volume 13, Issue 6, 2023, 534
https://doi.org/10.33263/BRIAC136.534

Investigation of the New Inhibitors by Modified Derivatives of Pinocembrin for the Treatment of Monkeypox and Marburg Virus with Different Computational Approaches

Shopnil Akash [1], Md. Rezaul Islam [1], Md. Mominur Rahman [1], Md. Saddam Hossain [2], Md. A.K. Azad [1], Rohit Sharma [3,*]

[1] Department of Pharmacy, Faculty of Allied Health Sciences, Daffodil International, University, Dhaka, Bangladesh
[2] Department of Biomedical Engineering, Faculty of Engineering & Technology, Islamic University, Kushtia, Bangladesh
[3] Department of Rasa Shastra and Bhaishajya Kalpana, Faculty of Ayurveda, Institute of Medical Sciences, Banaras Hindu University, Varanasi-221005, Uttar Pradesh, India
* Correspondance: Rohit Sharma: rohitsharma@bhu.ac.in (R.S.);

Scopus Author ID 57212897459
Received: 8.10.2022; Accepted: 13.11.2022; Published: 6.02.2023

Abstract The widespread occurrence of Monkeypox and Marburg virus fatalities all over the globe has prompted biologists, pharmacologists, chemists, and pharmacists to develop potent drug agents. This study generated eight compounds from pinocembrin derivatives by adding different functional groups to identify new effective drugs against Monkeypox and Marburg virus. Before the computational screening, they were optimized by material studio 08 in Density Functional Theory (DFT). Then, the "Highest Occupied Molecular Orbital" (HOMO), and the "Lowest Unoccupied Molecular Orbital" (LUMO) were analyzed, which further turned into the measurement of the chemical reactivity such as E(gap), hardness, softness, electronegativity, index, and chemical potential, between them. All the compounds were documented to have a greater hardness and softness index. After that, sequentially, Lipinski rule analysis, molecular docking, acute toxicity, acute systemic toxicity, Quantitative Structure-Activity Relationships (QSAR), and PASS prediction were all performed on these molecules to establish a potent medication. Firstly, the PASS prediction spectrum was taken, and these derivatives are highly potent antiviral compared with antibacterial, antifungal, and antidiabetics. The binding energy was determined using the PyRx AutoDock vina technique to identify the intermolecular protein-ligand couplings. The presentable maximum binding affinities were -9.0 kcal/mole against the Monkeypox virus (PDB ID 4QWO), and the top score against the Marburg virus (PDB 4OR8) was *-8.3* kcal/mole. The pIC_{50} score ranges from 4.44 to 4.44 for the reported molecules. Finally, the pharmacokinetics showed that most of the ligands are free from carcinogenic effects, have better absorbance capability, have low to moderate aqueous solubility, and are ligands 01, 03, 04, 05, and 08 might penetrate the blood-brain barrier (BBB). The pinocembrin derivatives exhibited significant structural and pharmacological features and can be used as prospective antiviral medicines for Monkeypox and Marburg viruses. However, a more experimental investigation is required on a broad scale to establish them as commercial medications.

Keywords: Monkeypox virus; Marburg virus; molecular docking; DFT; PASS prediction; ADMET; QSAR.

1. Introduction

In 1958, an epidemic of a vesicular disease among captive monkeys brought from Africa to Copenhagen, Denmark, for research purposes led to the discovery of MPXV. Thus, the term "Monkeypox" was created [1, 2]. In sub-Saharan Africa, 47 cases of human Monkeypox were identified between 1970 and 1979 in the initial epidemiologic research. Of these, 38 instances were discovered in the Democratic Republic of the Congo, with the remaining cases appearing in Cameroon, the Central African Republic, Gabon, Nigeria, and Sierra Leone[3]. Although human Monkeypox infections have historically occurred in West Africa, the Congo Basin of Central Africa has recorded the majority of cases since 1981[4, 5]. Laboratories employees in Frankfurt, Germany, Marburg, Germany, and Belgrade, Yugoslavia (now Serbia), contracted an infection caused by a hitherto unidentified infectious pathogen in August 1967. Seven of the 31 individuals (25 with original infections and six with subsequent infections) acquired a deadly condition. A retrospective diagnosis was made in another case that displayed illness symptoms [6]. African green monkeys (*Chlorocebus aethiops*), which were brought from Uganda and transported to all three locations, were found to be the cause of the virus. Ironically, the main infections happened when the monkeys' kidney cells were removed from them in order to develop poliomyelitis vaccine strains. Scientists from Marburg and Hamburg worked together to isolate, characterize, and identify the causative agent in a remarkable period of fewer than three months [7, 8]. Kunz and colleagues [9] and Kissling and colleagues [10] later corroborated this work. The disease, which marked the first isolation of a filovirus, was known as the Marburg virus after the city with the highest incidence. The earliest report on the causal agent of Marburg virus disease has frequently been incorrectly attributed to a study that claimed the enigmatic sickness was brought on by rickettsia or chlamydia [11].

When the third wave of SARS-CoV-2 is going on around the globe, another pandemic is knocking at the door, which has been happening due to Monkeypox and Marburg virus [12, 13]. The Monkeypox virus is a DNA virus responsible for infecting global people in recent times. The most common places to find Monkeypox are in the west and central Africa; nevertheless, the virus has recently been found in various non-endemic locations outside of Africa, prompting plenty of alarm [14-17]. Since May 13, 2022, the World Health Organization (WHO) has received reports of or identified 780 laboratory-confirmed cases of Monkeypox from 27 Member States spread throughout four WHO regions that are not prevalent for the Monkeypox virus. As of June 2, 2022, these cases originated from 27 countries. Investigations into epidemiology are still going on [18]. Besides, The Marburg virus disease is a kind of catastrophic hemorrhagic fever that may be transmitted between humans and non-human species [19-21]. This pathogenic virus is a filovirus belonging to the family of RNA viruses known as filoviruses [22]. On July 7, 2022, the Ministry of Health in Ghana recognized two fatal instances of what they believe to be the Marburg virus disease in two distinct places within the Ashanti Region. Both occurrences occurred in people who had been infected with Marburg virus disease. Since then, policymakers worldwide have been concerned about this infection [22]. Although these two pathogens (Monkeypox and Marburg virus) pose a great health concern around the globe, there is no effective cure or potential treatment. Pinocembrin, also known as 5, 7-dihydroxy flavanone, is the flavonoid group of molecules available in natural sources and has numerous biological benefits such as antioxidant, antibacterial, antiviral, and anti-inflammatory functionalities [23, 24]. Therefore, the purpose of this present research was to investigate the antiviral effect in consequences of pinocembrin and its modified or synthetic

compounds by adding different functional groups, including Benzene ring and -OH, COOH, Cl, F, Br, I, NO_2, and CH_3. In this case, the computational method has been performed to minimize time, cost, labor, and effort. Because more than $985 million cost is required, and also 10-15 years to develop a medication [25], however, using computational techniques, we can save the risk of cost, human resources, and time and provide leads to future researchers in drug development.

2. Experimental methodology

2.1. Pass prediction.

The development of new drug molecules has been considered complicated and challenging work. So, the pass perdition spectrum may be a valuable tool for primary screening of identifying potentiality against specified pathogens which may provide a broad range of biological targets and may be conceptualized based on the relatively intricate and varied chemical properties [26]. The PASS online tool offers the capability to make predictions for 3678 potent biological consequences, as well as the mechanisms and exceptional toxicities of the chemical, such as mutagenicity, carcinogenicity, teratogenicity, and embryotoxicity, and it is shown by Pa and Pi score [27]. The maximum probability of active (Pa) and probability of inactive (Pi) score has been considered 1 Pa > Pi. A more excellent Pa score has a higher chance of being active, and a lower Pi score has a more significant opportunity to be inactive. The data was obtained in the URL mentioned (http://way2drug.com/PassOnline/predict.php)[28].

2.2. Determination of ADMET, Lipinski rule, and pharmacokinetics.

Before the development of these modern technologies, many drug candidates failed after clinical trials due to life-threatening adverse impacts on humans. But, now, online and computational ADMET (absorption, distribution, metabolism, excretion, and toxicity) prediction reduces these chances since the ADMET profile may be obtained early stages of drug development. So, the ADMET data has been measured from the online web tool pkCSM (http://biosig.unimelb.edu.au/pkcsm/), which provided a vast number of pharmacological properties such as water solubility, human intestinal absorption, blood-brain barrier (BBB) permeability, CYP450 1A2 Inhibitor,CYP450 2C9 inhibitor, total clearance, Caco-2 permeability, andAMES toxicity, Max. tolerated dose and hepatotoxicity, and they ensure a drug candidate's safety profile.

2.3. Preparation of ligand and molecular optimization.

Chem Bio Draw 12.0.02 has been performed to create the 2D modification structures of pinocembrin as ligands and exported as mole form in the specified folder of the desktop. Then, Chem Bio 3D 12.0.02 software was used to transform 2D to 3D illustrations, and these were then reduced in energy using a technique developed in the same program and stored in SDF format. Figure 2 and Figure 3 display the 2D and 3D structures of all ligands. Afterward, each structure was optimized using the material studio 08application by density functional theory (DFT) from the DMol code. The B3LYP functional and the 6-31G++ were utilized effectively in the DMol code to achieve the exact result. Then, Frontier molecular orbital, highest occupied molecular orbital – lowest unoccupied molecular orbital (HOMO-LUMO) was measured[29]. In the end, the optimized geometries were documented as protein databank

PDB files to be employed as substrates in molecular docking, ADMET, and another related computational experiment. The given formula has been used to measure quantum properties energy gap (E gap), chemical potential (μ), electronegativity (χ), hardness (η), and softness (S) through the DFT approach[30].

$$E_{gap} = (E_{LUMO} - E_{HOMO}) \ldots\ldots\ldots\ldots\ldots\ldots\ldots\ldots\ldots\ldots (1)$$

$$I = -E_{HOMO} \ldots\ldots\ldots\ldots\ldots\ldots\ldots\ldots\ldots\ldots\ldots\ldots\ldots\ldots (2)$$

$$A = -E_{LUMO} \ldots\ldots\ldots\ldots\ldots\ldots\ldots\ldots\ldots\ldots\ldots\ldots\ldots\ldots (3)$$

$$(\chi) = \frac{I + A}{2} \ldots\ldots\ldots\ldots\ldots\ldots\ldots\ldots\ldots\ldots\ldots\ldots\ldots\ldots (4)$$

$$(\mu) = -\frac{I + A}{2} \ldots\ldots\ldots\ldots\ldots\ldots\ldots\ldots\ldots\ldots\ldots\ldots\ldots\ldots (5)$$

$$(\eta) = \frac{I - A}{2} \ldots\ldots\ldots\ldots\ldots\ldots\ldots\ldots\ldots\ldots\ldots\ldots\ldots\ldots (6)$$

$$(\sigma) = \frac{1}{\eta} \ldots\ldots\ldots\ldots\ldots\ldots\ldots\ldots\ldots\ldots\ldots\ldots\ldots\ldots (7)$$

2.4. Protein preparation and Molecular docking study and visualization

The microstructures of the Monkeypox virus (PDB ID 4QWO) and Marburg virus (PDB 4OR8) were instantaneously acquired from the PDB (protein data bank) from this URL (http://www.rscb.org/pdb) in pdb format. Then, the macromolecular protein was purified by Pymol 2020 to get fresh protein. The resolution and three-dimensional structure of fresh protein have been displayed in Fig.1. When the protein and ligand were prepared, the virtual screening was conducted by implementing PyRx AutoDock vina for molecular docking[31].

Monkeypox Virus (PDB ID 4QWO)
Organism: Monkeypox virus Zaire-96-I-16
Method: X-ray diffraction
Resolution: 1.52 Å

Marburg virus (PDB 4OR8)
Organism: Marburg virus - Musoke, Kenya, 1980
X-ray diffraction
Resolution: 2.65 Å

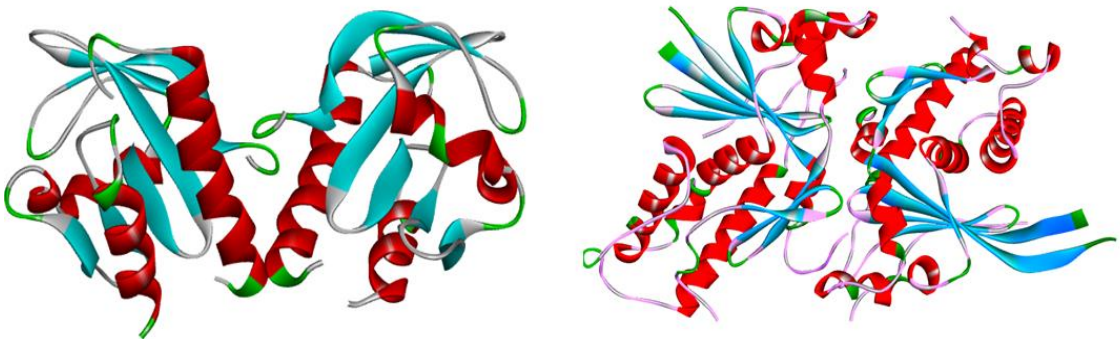

Ref.[32] Ref. [33]

Figure 1. Three-dimensional protein structure of Monkeypox and Marburgvirus.

2.5. Determination of Lipinski rule.

Typically, therapeutic and active oral medications have followed different rules to establish operational and potent medicines. Lipinski's rule of five is one of the vital investigations of molecules to make them for oral use, which is followed by (i.e., a molecule with a molecular mass less than 500 Da, no more than five hydrogen bond donors, no more than ten hydrogen bond acceptors, and an octanol-water partition coefficient log P not greater

than 5). When any molecules follow this typical Lipinski's rule of five, they should be considered oral and active drugs. Lipinski's score of five was obtained from the Swiss ADME online tool, which may access by following (http://www.swissadme.ch/index.php).

2.6. QSAR data calculation (pIC_{50}).

QSAR, or quantitative structure-activity relationship, is a computer modeling technique for elucidating connections between the structural features of chemical substances and their biological functions. QSAR modeling is crucial in the search for new therapeutics. To get over limitations and provide accurate forecasts, a mathematical method has been deployed, which was developed and reported by previous research. Before that, required data were taken from ChemDes (www.scbdd.com/chemdes/) server ". Then, the data obtained were put into multiple linear regression (MLR) and the pIC_{50}. The mentioned MLR equation was used, which is obtained from previous research[34, 35]; here, pIC_{50} (Activity) = − 2.768483965 + 0.133928895 × (Chiv5) + 1.59986423 × (bcutm1) + (− 0.02309681) × (MRVSA9) + (− 0.002946101) × (MRVSA6) + (0.00671218) × (PEOEVSA5) + (− 0.15963415) × (GATSv4) + (0.207949857) × (J) + (0.082568569) × (Diametert) and obtained the pIC_{50}[36].

3. Results and Discussion

3.1. Structural activity relationship (SAR) studies.

Structure-Activity Relationship, abbreviated as SAR, is a method that aims to discover correlations between the chemical structure (or structural-related characteristics) of researched metabolites and the bioactivity (or target attribute) of such biomolecules. In these studies, the primary compound was pinocembrin, a significant flavonoid component integrated as a multifunctional pharmacological effect such as antimicrobial, anti-inflammatory, antioxidant, and anticancer activities [37]. So, the most abundant functional group, such as the Benzene ring and -OH, COOH, Cl, F, Br, I, NO_2, and CH_3, have been picked up and substituted in the hydroxyl group of aromatic rings. In addition, computational screening has been conducted to measure how pharmacological effects change in functional groups.

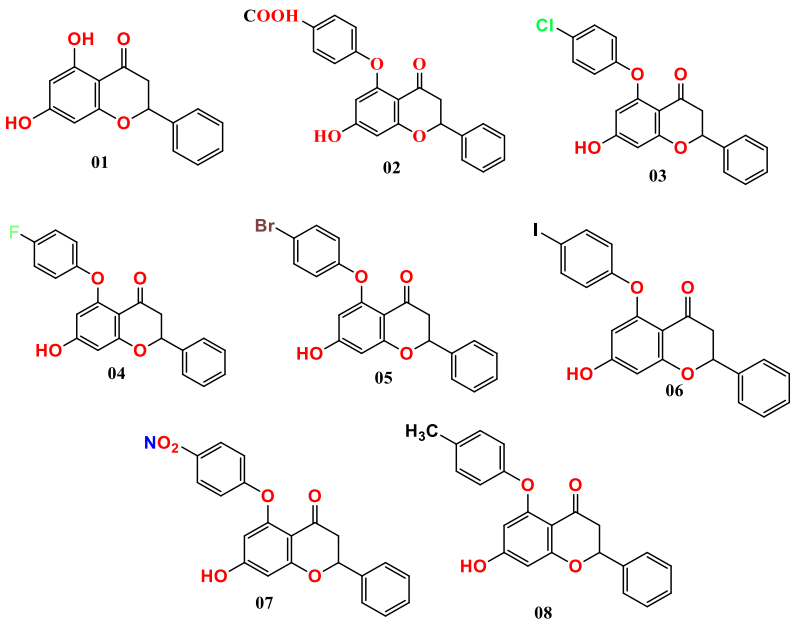

Figure 2. Chemical structure of Pinocembrin and its derivatives.

3.2. Optimized structure of the tested ligand.

Molecular optimization plays molecules' most essential and fundamental features, making them stable [38]. The three-dimensional distribution of individual molecules may be predicted using a technique known as geometry optimization. This technique involves the reduction of a model's electric potential. According to a working hypothesis, the effects of binding energy, which is to suggest that stable frameworks are formed by the clustering of smaller structures and may be described by geometry optimization. The optimization has been performed in this investigation by material studio 08 software, and graphically the three-dimensional individual optimized molecules have been written in Figure 3.

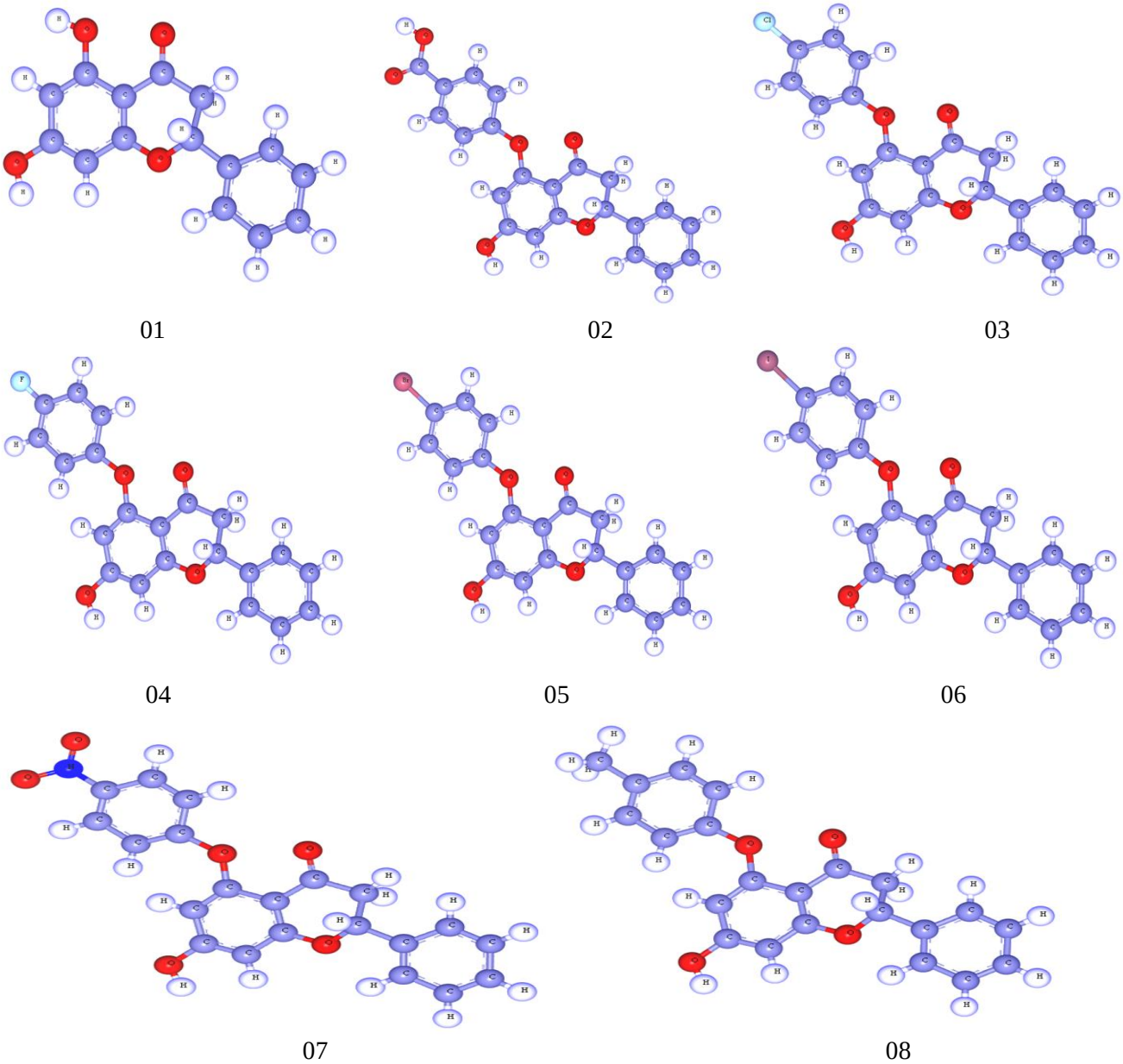

Figure 3. Optimized structure of Pinocembrin and its derivatives.

3.3. Evaluation of antiviral efficacy (PASS Prediction) activity.

Pass prediction is the initial investigation of bioactive molecules' efficacy, represented by the probability of active (Pa) and probability of inactive (Pi). More Pa value and less Pi score have a greater chance of being potent, while Pa and Pi will never equal. Bioactive components may have curative benefits as well as additional effects, the latter of which are

known as side effects. So, these innovative features of the molecules should be predicted in the early stages and easily understand the potency of any molecules. In Table 1, it is reported that the Pa score is about 0.608 -0.519 for the virus, 0.239 – 0.395 for bacteria, 0.484 – 0.582 for fungi, and 0.194 – 0.345 for antidiabetics. So, the ranges of Pa scores are much greater for antiviral compared with antibacterial, antifungal, and antidiabetic. Based on this predicted Pa score, Monkeypox, and Marburgvirus have been picked up to make a potent drug and a strong inhibitor against them.

Table 1. Data of pass prediction data.

Ligand No	Antiviral (Influenza)		Antibacterial		Antifungal		Antidiabetic	
	Pa	Pi	Pa	Pi	Pa	Pi	Pa	Pi
01	0.608	0.005	0.395	0.031	0.582	0.020	0.214	0.147
02	0.584	0.008	0.382	0.030	0.536	0.025	0.345	0.062
03	0.575	0.009	0.239	0.089	0.550	0.024	0.272	0.099
04	0.532	0.015	0.253	0.081	0.522	0.027	0.269	0.101
05	0.532	0.015	0.287	0.065	0.526	0.044	0.249	0.114
06	0.532	0.015	0.313	0.055	0.484	0.033	0.194	0.134
07	0.519	0.019	0.338	0.047	0.541	0.025	0.241	0.083
08	0.571	0.009	0.296	0.062	0.536	0.025	0.258	0.108

3.4. Lipinski rule and pharmacokinetics.

The goal of Lipinski's Rule of Five (RO5) has been conducted to evaluate and utilize in the design of pharmacological molecules that are acceptable and suitable for oral medication based on biological and physiochemical similarities[39]. In this investigation, the predicted molecular weight of the compounds is 256.25 Dalton - 458.25 Dalton, the number of rotatable bonds, 01 – 04, hydrogen bond acceptor 04-06, hydrogen bond donor 01-02, and the ranges of topological polar surface area are 55.76 Å² - 101.58 Å² and the Consensus Log is about2.26 – 4.36 which all are within the rages of Lipinski's rule of five (RO5) and followed the guideline of Lipinski's Rule of Five (RO5) where no violation was not seen for any molecules. In the last point of view, the Bioavailability Score has been seen at 0.55 in most cases, but sometimes 0.56 is also seen in compound 02. Accordingly, in Lipinski's RO5, all the medications may serve as a foundation for testing as novel oral medications.

Table 2. Data of Lipinski rule, pharmacokinetics.

Ligand No	Molecular weight	Number of rotatable bonds	Hydrogen bond acceptor	Hydrogen bond donor	Topological polar surface area Å²	Consensus Log $P_{o/w}$	Lipinski rule		Bioavailability Score
							Result	violation	
01	256.25	01	04	02	66.76	2.26	Yes	00	0.55
02	376.36	04	06	02	93.06	3.26	Yes	00	0.56
03	366.79	03	04	01	55.76	4.22	Yes	00	0.55
04	350.34	03	05	01	55.76	4.0	Yes	00	0.55
05	411.25	03	04	01	55.76	4.32	Yes	00	0.55
06	458.25	03	04	01	55.76	4.36	Yes	00	0.55
07	377.35	04	06	01	101.58	2.95	Yes	00	0.55
08	346.38	03	04	01	55.76	4.01	Yes	00	0.55

3.5. Molecular docking and interaction analysis against Monkeypox and Marburg virus.

According to the finding of the pass prediction score, the antiviral Pa score was the maximum. So, it is fascinating that this pinocembrin derivative could be effective against Monkeypox and Marburgvirus. So, based on this hypothesis, Monkeypox and Marburgvirus have been included in this investigation.

It is thought that any active biological molecules could potentially produce pharmacological effects if their minimum binding energy is -6.0kcal/mole[40, 41]. The finding docking score against the Monkeypox virus was found to be -9.0 kcal/mol, -8.8 kcal/mol, and -8.7 kcal/mol as the maximum Monkeypox virus (PDB ID 4QWO), while the maximum score against the Marburg virus (PDB 4OR8) was reported -7.4 kcal/mole to -8.3 kcal/mole. Similarly, the standard (acyclovir) is displayed at -7.0 kcal/mole and -6.0 kcal/mole.

The FDA (food and drug administration) approved medication acyclovir has been included in this study to compare newly developed molecules. But it is seen that the docking score of acyclovir is much lower against Monkeypox and Marburgvirus than the pinocembrin derivatives. So, this medicine could perform better pharmacological effects than standard acyclovir if commercially available after synthesis and clinical trials.

Table 3. Binding Affinity against Monkeypox and Marburg virus.

Drug Molecules No	Monkeypox virus (PDB ID 4QWO)	Marburg virus (PDB 4OR8)
	Binding Affinity(kcal/mole)	Binding Affinity(kcal/mole)
01	-7.5	-7.4
02	-9.0	-8.0
03	-8.4	-8.1
04	-8.8	-8.3
05	-8.4	-8.0
06	-8.4	-8.1
07	-8.5	-8.0
08	-8.7	-8.3
Standard (Acyclovir)	-7.0	-6.0

3.6. Molecular docking pose and interaction analysis against Monkeypox and Marburg virus.

The Molecular docking pose and interaction analysis have been performed to evaluate the binding region of the drug-protein and how many active sides are present after the formation of the complex. This part of the investigation includes docking interactions between the proposed compound against Monkeypox and Marburg virus, hydrogen bonding, and a 2D picture of active sites. The drug-protein interaction and active sides displayed different active amino acid residues formed with different types of bonds like Conventional Hydrogen Bonds, Carbon hydrogen bonds, Pi-Pi stacked, and Pi-Alkyl bonds. The figures have been drawn based on the maximum docking score and are graphically represented A-:9. SER A: 12, ILE A: 35, active amino acid residues are formed in most cases of Monkeypox virus with proposed ligands, whereas LEU B: 223, MET B: 195, ASN B: 171, ASP B: 172, VAL B: 193 is formed drug with Marburg virus. The supplementary table S1 is shown the total amino acid residues of drugs with reported proteins. Besides Figure 4 (b) hydrogen bonding region, sky blue colors are displayed by the H-Bond donor region, and the H-Bond acceptor region determines the red color. In most cases, the H-Bonding acceptor region is more significant. So, they might be readily accepted hydrogen during the chemical reaction.

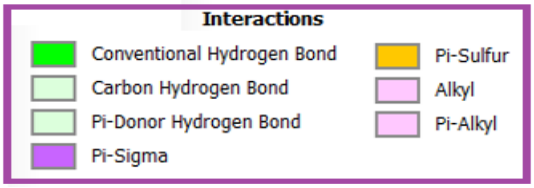

4a) Docking pocket 4b) Hydrogen bonding 4c) 2D picture of ligand and protein interaction

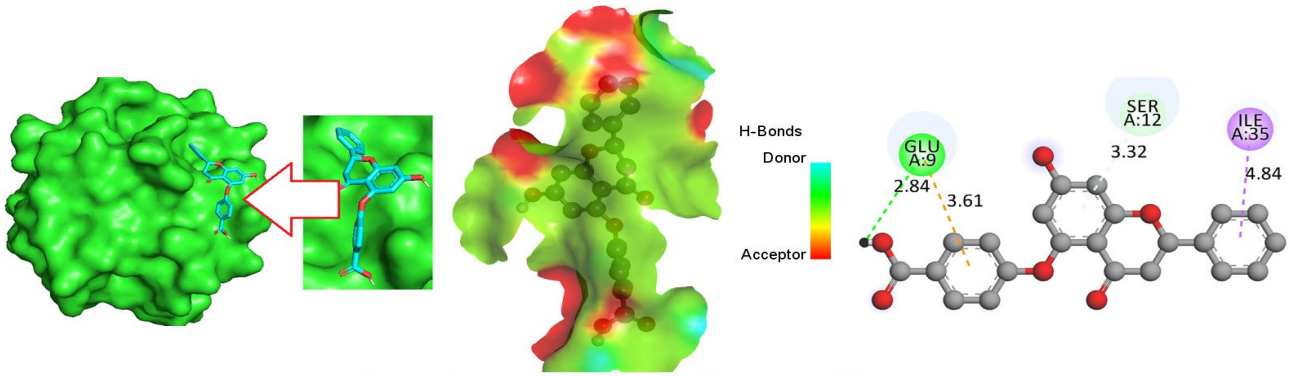

Molecular docking poses of *Monkeypox Virus (PDB ID 4QWO)* with Ligand 02

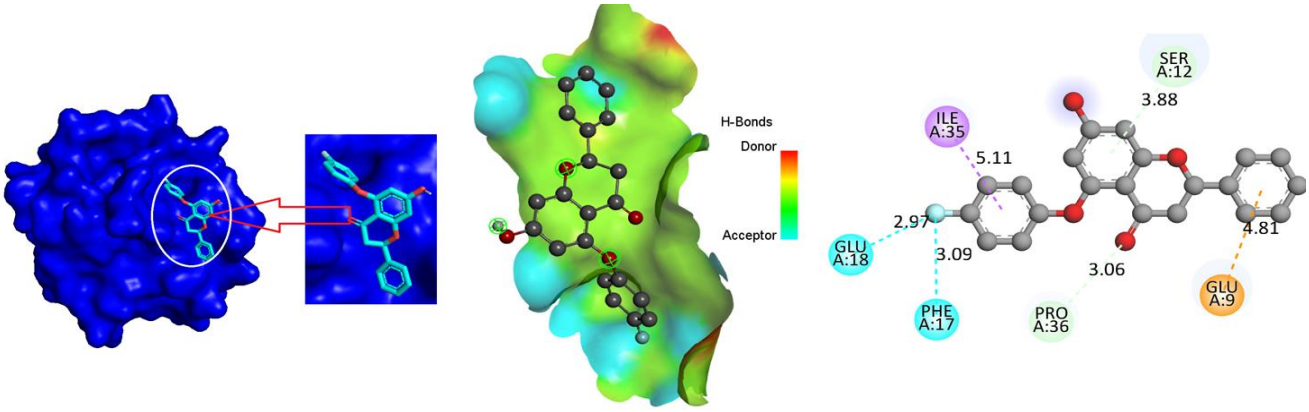

Molecular docking poses of *Monkeypox Virus (PDB ID 4QWO)* with Ligand 04

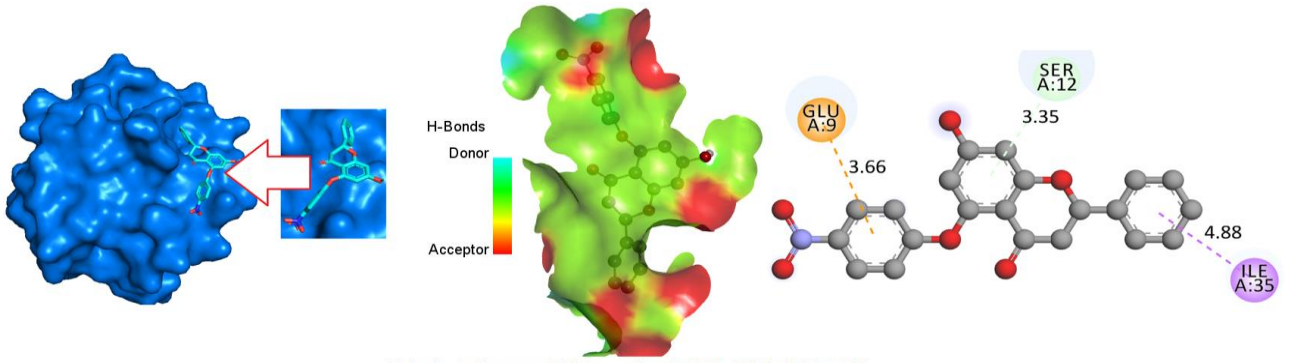

Molecular docking poses of *Monkeypox Virus (PDB ID 4QWO)* with Ligand 07

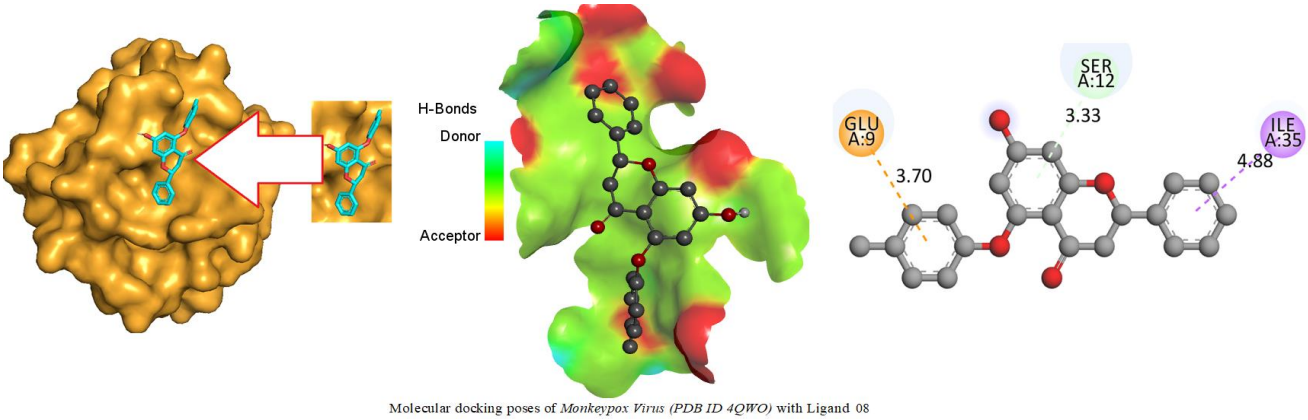

Molecular docking poses of *Monkeypox Virus (PDB ID 4QWO)* with Ligand 08

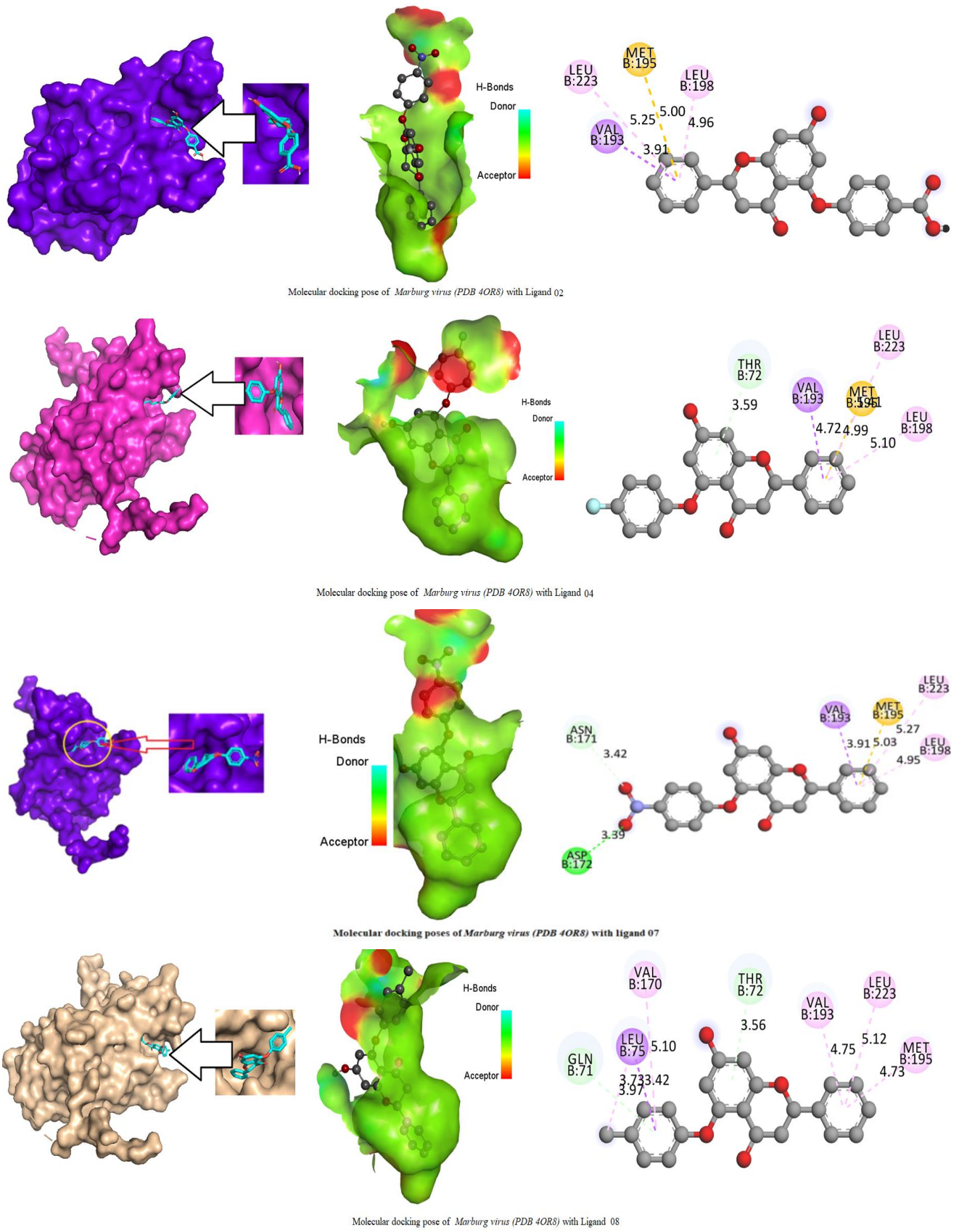

Figure 4. Docking interactions between the proposed compound and Monkeypox, Marburg virus, hydrogen bonding, and 2D picture of active sites.

3.7. Frontier Molecular Orbitals and Chemical Reactivity Descriptor.

Chemical descriptors have a specific meaning for any physiologically active molecule or bioactive compound, which has significant application from a drug designing perspective.

In our investigation, quantum chemical descriptors (εLUMO, εHOMO) were calculated by the DFT function from material studio 08[42]. After that, using a mathematical equation, the energy gap (Δε), chemical potential (μ), electronegativity (χ), hardness (η), and softness (σ) of the eight pinocembrin derivatives were measured and listed in Table 4. It is noted that the lower the HOMO LUMO gap greater the chance of being stabled[43]. The reported molecules found that ligands 03 & 06 have a 5.998 and 7. 396 energy gap, which is much lower than others, and they are better chemical reactivity[44]. The chemical potential and electronegativity are also crucial during chemical reaction formation. Besides, the greater hardness requires a higher force to break down, whereas the more sumptuous softness can dissolve or break down rapidly. Our finding reported that ligands 03 and 05 have lower hardness and better softness than ligands 01,02,04, 05,07, and 08. So, ligands 03 and 05 may easily break down after reaching physiological systems. But, the ligands 01,02,04, 05,07 may have required more time to break down.

Table 4. Chemical reactivity descriptor data.

S/N	A=-LUMO	I=-HOMO	Energy Gap E(gap) =I-A	Chemical potential $(\mu) = -\frac{I+A}{2}$	Electronegativity $(\chi) = \frac{I+A}{2}$	Hardness $(\eta) = \frac{I-A}{2}$	Softness $(\sigma) = \frac{1}{\eta}$
01	-0.904	-9.893	8.989	5.398	-5.398	4.494	0.2225
02	-0.998	-9.913	8.915	5.455	-5.455	4.457	0.2243
03	-0.990	-6.988	5.998	3.989	-3.989	2.999	0.3334
04	-1.050	-9.105	8.055	5.077	-5.077	4.027	0.2483
05	-0.991	-8.387	7.396	4.689	-4.689	3.698	0.2704
06	-1.910	-4.538	8.055	5.077	-5.077	4.027	0.2483
07	-1.096	-9.919	8.823	5.507	5.507	4.411	0.2267
08	-0.979	-9.902	8.923	5.440	-5.440	4.461	0.2261

3.8. Frontier molecular orbitals (HOMO and LUMO) diagram.

The Frontier Molecular Orbitals (HOMO and LUMO) diagram was illustrated by DFT [45, 46]. The maximal electron density concentration in the chemical compound segment that an electrophile may quickly attack is referred to as the HOMO segment. From the pictures, the red and green color segment is designed by the HOMO region [47]. Besides, the LUMO segments are designed in a blue and yellow hue. LUMO denotes the lack of electrons where a nucleophilic species may be easily replaced. It is evident that drug molecules might be attached to the LUMO segments [48, 49]. The Frontier Molecular Orbitals diagram is displayed in Figure 5.

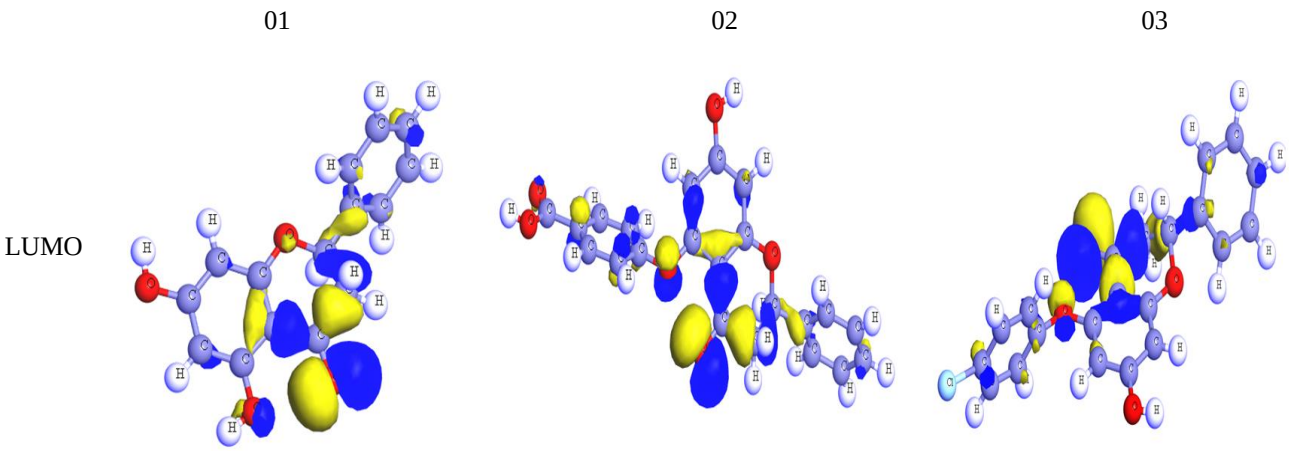

HOMO

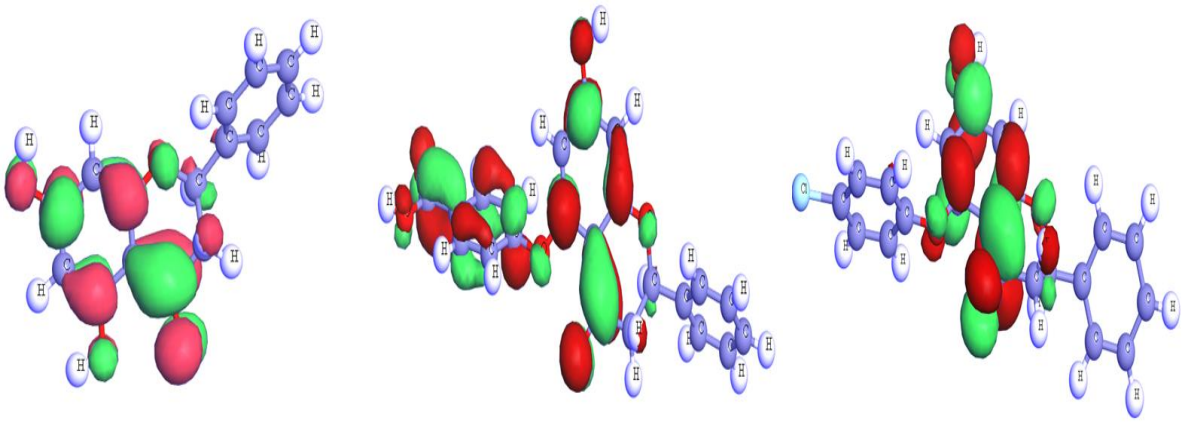

04 05 06

LUMO

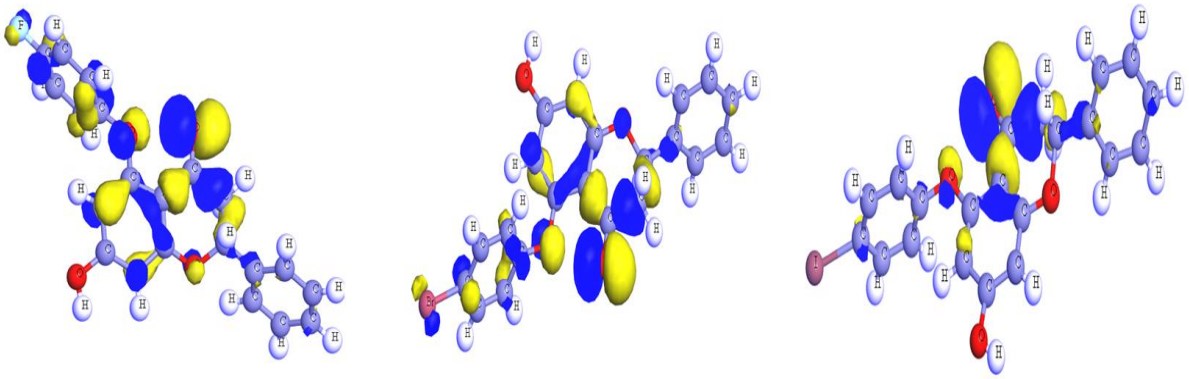

HOMO

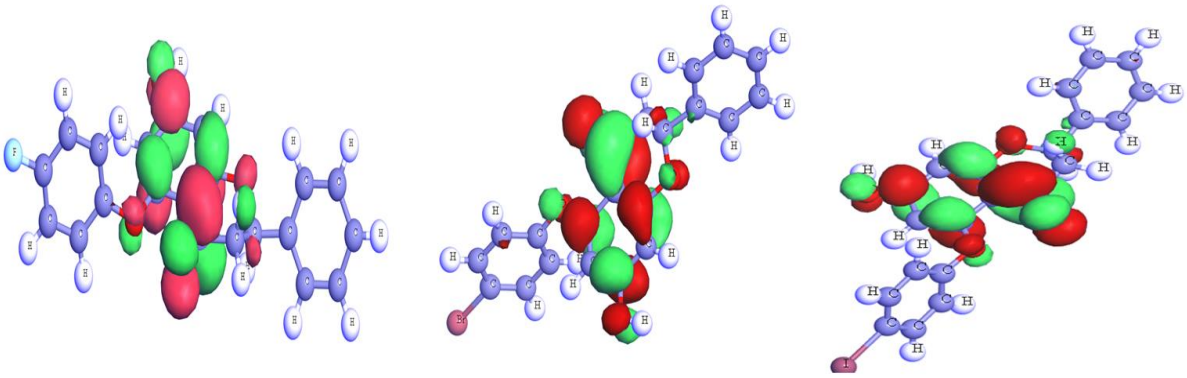

07 08

LUMO

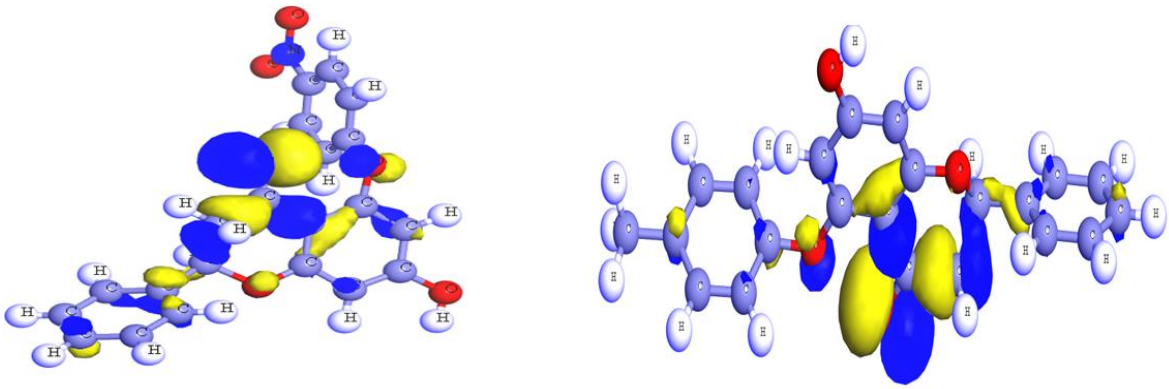

HOMO

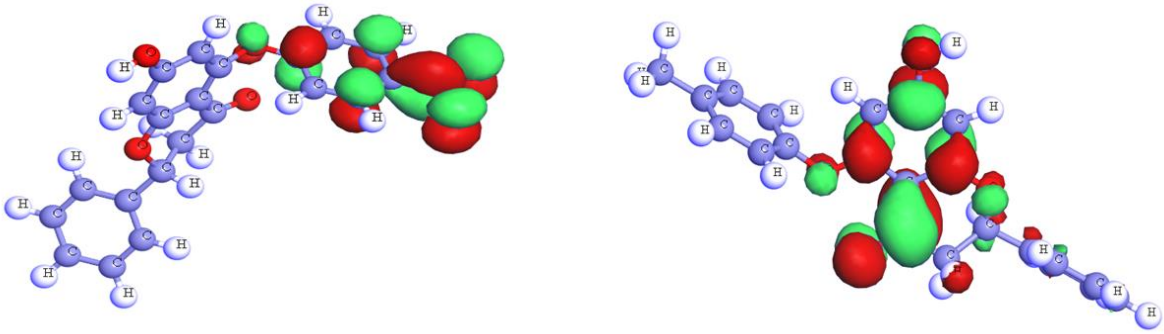

Figure 5. A frontier molecular orbitals diagram is displayed.

3.9. ADMET data investigation.

Even though an inhibitor or bioactive compound has an agonistic reaction when it binds to a targeted pathogenic protein receptor or an enzyme, this does not always mean that it might develop into a proper or suitable medication if it fails in ADMET investigation [50]. A large percentage of active and potent drugs fail to work in clinical trials due to a lack of pharmacodynamics (ADME) qualities, which may cause severe damage to physiological systems. Consequently, ADME (absorption, distribution, metabolism, and excretion) analysis and drug-likeness investigation have been significant in drug development since they improve the proper choice about whether or not to investigate compounds have safety and efficacy in the physiological system and aquatic non-aquatic environment. So, the computational prediction of ADME has been listed. The water solubility (Log S) standard score in ADME data is assumed from -4 to -6 and -2 to -4 for minimum and maximum solubility substances[51]. In this current investigation, water solubility (Log S) ranges are predicted as -3.485 in Ligand 01 and -2.892 in Ligand 05. In contrast, the remaining compounds are predicted to be greater than -4, representing that ligands 01 and 05 are maximum solubility and other ligands are minimum solubility. The Caco-2 Permeability ranges are about 0.27 to 1.455, and Intestinal absorption (human) (%) has been reported to be 73.515% - 98.954%, and it is described that they are highly absorbed in the GI tract[52, 53]. The substitute of different functional groups continuously increases the volume of distribution, and maximum VDss is reported at -0.930 Log L/kg in addition to the carboxylic group. The BBB permeability has positively occurred in most ligands (01, 03, 04, 05, and 08).

Table 5. ADME features computation.

S/N	Absorption			Distribution		Metabolism		Excretion	
	Water solubility (Log S)	Caco-2 Permeability (10^{-6} cm/s)	Intestinal absorption (human) (%)	VDss (human) (log L/kg)	BBB permeability	CYP450 1A2 Inhibitor	CYP450 2C9 Inhibitor	Total Clearance (ml/min/kg)	Renal OCT2 substrate
01	-3.485	1.185	91.639	-0.181	No	Yes	No	0.148	No
02	-4.253	0.917	73.515	-0.930	No	No	Yes	0.431	No
03	-5.50	1.114	90.977	-0.601	Yes	Yes	Yes	0.074	No
04	-4.995	1.168	92.03	-0.827	Yes	Yes	Yes	0.092	No
05	-2.892	0.27	81.538	0.011	Yes	Yes	No	-0.494	No
06	-5.551	1.11	91.546	-0.576	Yes	No	Yes	-0.236	No
07	-5.456	1.455	98.954	-0.905	No	No	Yes	0.202	No
08	-4.776	1.383	93.551	-0.512	Yes	Yes	Yes	0.206	No

On the other hand, the CYP450 1A2 Inhibitor and metabolic enzyme may be inhibited by (01, 03, 04, 05, and 08), while the CYP450 2C9 Inhibitor may be inhibited by (02, 03, 04, 06, 07, and 08). The last one is Total Clearance which found the ranges 1.48 to 0.431 as positive, and Ligand 05 and 06 found negative scores from -0.236 to -0.494. Finally, no drugs can substitute for Renal OCT2 substrate.

3.9. Aquatic and non-aquatic toxicity.

The aquatic and non-aquatic toxicity has been conducted to determine what effects should impact the physiological after-administration system and environment after exposure during manufacturing or after excreting from human waste[54]. So, the first thing we have measured is AMES toxicity, which reflects that Ligand 05 and 07 should produce cariogenic impact while Ligand 02, 04, and 07 may produce hepatotoxicity. So, before using this specified medication, one should be conscious and ensure all the ligands are free from skin sensitization. Secondly, Max. tolerated dose range is found to be 0.390 mg/kg/day – 0.750 mg/kg/day, while the Oral Rat Acute Toxicity (LD50) ranges is reported to be 1.95 mole/kg to 2.577, and Oral Rat Chronic Toxicity ranges are about 1.096 mg/kg/day - 21.92 mg/kg/day. So, the overall investigation has reflected that almost all the ligands are human useable, and only a few drugs may produce AMES and hepatotoxicity.

Table 6. Aquatic and non-aquatic toxicity value prediction.

S/N	AMES toxicity	Max. tolerated dose (human) mg/kg/day)	Oral Rat Acute Toxicity (LD50) (mol/kg)	Oral Rat Chronic Toxicity (mg/kg/day)	Hepatotoxicity	Skin Sensitization
01	No	0.651	1.95	1.949	No	No
02	No	0.579	2.64	1.378	Yes	No
03	No	0.578	2.549	1.11	No	No
04	No	0.750	2.577	1.236	Yes	No
05	Yes	0.438	2.482	21.92	No	No
06	No	0.574	2.572	1.096	No	No
07	Yes	0.390	2.501	1.142	Yes	No
08	No	0.499	2.536	1.671	No	No

3.10 QSAR and PlogIC$_{50}$

The quantitative structure-activity relationship (QSAR) is a computational and mathematical equation describing therapeutic molecules' biological activity. The mathematical QSAR model was working of multiple linear regression, which had been built in Excell shit by analyzing the computational IC50 values similar to pIC50 [-log (IC50)]. From the ChEMBL open-source website[55]. ChEMBL was developed by more than a million bioactive molecules and was founded from the eight most approved biological characteristics, including hiv5, bcutm1, MRVSA9, MRVSA6, PEOEVSA5, GATSv4, J, and diameter, among others[56, 57].

Moreover, the IC50 values are closely correlated to its structural chain, and this value changes with the modification in its side chain. The score of IC50 increases as the molecular weights of the medicine increase, but it must remain under 10.00 to be considered an efficient medication. As mentioned, the Table 7, it has been reported that the pIC50 is 4.44 to 4.44. It has been established that the range of pIC50 ratios for standard and effective medications should be 4.0 – 10[58]. So, the pIC50 value of drugs (01- 08) is acceptable as a standard drug since the value is not more than 10.0.

Table 7. Data commutate of QSAR.

Ligand	Chiv5	bcutm1	(MRVSA9)	(MRVSA6)	(PEOEVSA5)	GATSv4	J	Diametert	PIC50
1	1.535	3.948	5.783	53.591	3.332	0.916	1.675	9	4.61
2	2.172	3.971	11.753	83.42	30.332	0.932	1.366	15	4.44
3	2.205	3.985	17.384	82.88	41.933	0.947	1.399	14	4.83
4	2.08	3.969	5.783	83.674	30.332	0.832	1.399	14	5.01
5	2.341	6.842	21.773	82.33	46.262	0.806	1.399	14	4.37
6	2.435	10.673	28.374	81.487	30.332	0.655	1.399	14	5.08
7	2.153	3.972	11.471	87.971	30.332	0.937	1.366	15	5.22
8	2.183	3.969	5.783	83.42	48.028	0.947	1.399	14	6.89

4. Conclusions

This study's objective was to investigate effective and potent antiviral medication for Monkeypox and Marburg virus by adding different functional groups in the side chain of pinocembrin. So, pinocembrin was picked up as a primary compound and substituted with one hydroxyl group of pinocembrin by a different functional group. After that pass prediction spectrum (Pa) was evaluated, and maximum Pa was found for antiviral. So, based on the score of the Monkeypox and Marburg viruses were selected as targeted pathogens and performed numerous computational investigations, such as quantum calculation (HOMO-LUMO, energy gap, hardness, softness) by DFT method, likeness drug- and Lipinski rule, QSAR, ADMET, molecular docking, and dynamic simulation, etc. In these studies, the Pa score is about 0.608 - 0.519 for viruses, 0.239 – 0.395 for bacteria, 0.484 – 0.582 for fungi, and 0.194 – 0.345 for antidiabetics. So, the ranges of Pa scores are much greater for antiviral compared with antibacterial, antifungal, and antidiabetic; the ranges of pIC50 are 4.44 to 4.44, Max. tolerated dose range is found to be 0.390 mg/kg/day – 0.750 mg/kg/day, while the Oral Rat Acute Toxicity (LD50) ranges is reported to be 1.95 mole/kg to 2.577, and Oral Rat Chronic Toxicity ranges are about 1.096 mg/kg/day - 21.92 mg/kg/day. The predicted molecular weight of the compounds is 256.25 Dalton - 458.25 Dalton, the number of rotatable bonds, 01 – 04, hydrogen bond acceptor 04-06, hydrogen bond donor 01-02, and the ranges of topological polar surface area are 55.76 $Å^2$ - 101.58 $Å^2$ and the Consensus Log is about2.26 – 4.36 which all are within the rages of Lipinski's rule of five (RO5) and followed the guideline of Lipinski's Rule of Five (RO5) where no violation was not seen for any molecules. After comprehensive studies, it is found that all the medication is satisfied by the Lipinski rule, acceptable ranges of QSAR, better pharmacokinetics, and ADMET profile, and the most potent binding energy to inhibit the Monkeypox and Marburgvirus. The reported docking score was -9.0 kcal/mole, -8.8 kcal/mole, and -8.7 kcal/mole as the maximum against Monkeypox Virus (PDB ID 4QWO), and the maximum score against Marburgvirus (PDB 4OR8) was reported -7.4 kcal/mole to -8.3 kcal/mole. So, this study revealed that the reported medication could be a better choice against Monkeypox and Marburg virus, and future laboratory and clinical experiments are required.

Funding

No funding was received.

Acknowledgments

Authors acknowledge their respective departments.

Conflicts of authors

The authors declare no conflicts of interest.

References

1. Petersen, E.; Kantele, A.; Koopmans, M.; Asogun, D.; Yinka-Ogunleye, A.; Ihekweazu, C.; Zumla, A. Human monkeypox: epidemiologic and clinical characteristics, diagnosis, and prevention. *Infectious Disease Clinics* **2019**, *33*, 1027-1043, https://doi.org/10.1016/j.idc.2019.03.001.
2. Antunes, F.; Cordeiro, R.; Virgolino, A. Monkeypox: From A Neglected Tropical Disease to a Public Health Threat. *Infectious Disease Reports* **2022**, *14*, 772-783, https://doi.org/10.3390/idr14050079.
3. Weinstein, R.A.; Nalca, A.; Rimoin, A.W.; Bavari, S.; Whitehouse, C.A. Reemergence of Monkeypox: prevalence, diagnostics, and countermeasures. *Clinical infectious diseases* **2005**, *41*, 1765-1771, https://doi.org/10.1086/498155.
4. Reynolds, M.G.; Damon, I.K. Outbreaks of human Monkeypox after cessation of smallpox vaccination. *Trends in microbiology* **2012**, *20*, 80-87, https://doi.org/10.1016/j.tim.2011.12.001.
5. Chadha, J.; Khullar, L.; Gulati, P.; Chhibber, S.; Harjai, K. Insights into the Monkeypox virus: making of another pandemic within the pandemic? *Environmental Microbiology* **2022**, https://doi.org/10.1111/1462-2920.16174.
6. Slenczka, W.; Klenk, H.D. Forty years of Marburg virus. *The Journal of infectious diseases* **2007**, *196*, S131-S135, https://doi.org/10.1086/520551.
7. Siegert, R.; Shu, H.; Slenczka, H.; Peters, D.; Müller, G. The aetiology of an unknown human infection transmitted by monkeys (preliminary communication). *German medical monthly* **1968**, *13*, 1-2, https://pubmed.ncbi.nlm.nih.gov/4968593/.
8. Koundouno, F.R.; Kafetzopoulou, L.E.; Faye, M.; Renevey, A.; Soropogui, B.; Ifono, K.; Nelson, E.V.; Kamano, A.A.; Tolno, C.; Annibaldis, G. Detection of Marburg virus disease in Guinea. *New England Journal of Medicine* **2022**, *386*, 2528-2530, https://www.nejm.org/doi/full/10.1056/NEJMc2120183.
9. Kunz, C.; Hofmann, H.; Kovac, W.; Stockinger, L. Biological and morphological characteristics of the" hemorrhagic fever" virus occurring in Germany. *Wiener klinische Wochenschrift* **1968**, *80*, 161, https://pubmed.ncbi.nlm.nih.gov/5688605/.
10. Kissling, R.E.; Robinson, R.Q.; Murphy, F.A.; Whitfield, S.G. Agent of disease contracted from green monkeys. *Science* **1968**, *160*, 888-890, https://doi.org/10.1126/science.160.3830.888.
11. Smith, C.G.; Simpson, D.; Bowen, E.; Zlotnik, I. Fatal human disease from vervet monkeys. *The Lancet* **1967**, *290*, 1119-1121, https://www.thelancet.com/journals/lancet/article/PIIS0140-6736(67)90621-6/fulltext.
12. Okonji, O.C.; Okonji, E.F.; Mohanan, P.; Babar, M.S.; Saleem, A.; Khawaja, U.A.; Essar, M.Y.; Hasan, M.M. Marburg virus disease outbreak amidst COVID-19 in the Republic of Guinea: A point of contention for the fragile health system? *Clinical Epidemiology and Global Health* **2022**, *13*, 100920, https://doi.org/10.1016/j.cegh.2021.100920.
13. Mohapatra, R.; Sarangi, A.; Kandi, V.; Chakraborty, S.; Chandran, D.; Alagawany, M.; Chakraborty, C.; Dhama, K. Recent re-emergence of Marburg virus disease in an African country Ghana after Guinea amid the ongoing COVID-19 pandemic: Another global threat? Current knowledge and strategies to tackle this highly deadly disease having feasible pandemic potential. *International Journal of Surgery (London, England)* **2022**, *106*, 106863, https://doi.org/10.1016/j.ijsu.2022.106863.
14. Alakunle, E.; Moens, U.; Nchinda, G.; Okeke, M.I. Monkeypox virus in Nigeria: infection biology, epidemiology, and evolution. *Viruses* **2020**, *12*, 1257, https://doi.org/10.3390/v12111257.
15. Kumar, N.; Acharya, A.; Gendelman, H.E.; Byrareddy, S.N. The 2022 outbreak and the pathobiology of the monkeypox virus. *Journal of Autoimmunity* **2022**, 102855, https://doi.org/10.1016%2Fj.jaut.2022.102855.
16. Gigante, C.M.; Korber, B.; Seabolt, M.H.; Wilkins, K.; Davidson, W.; Rao, A.K.; Zhao, H.; Hughes, C.M.; Minhaj, F.; Waltenburg, M.A. Multiple lineages of Monkeypox virus detected in the United States, 2021-2022. *bioRxiv* **2022**, https://doi.org/10.1126/science.add4153.
17. Thornhill, J.P.; Barkati, S.; Walmsley, S.; Rockstroh, J.; Antinori, A.; Harrison, L.B.; Palich, R.; et al. Monkeypox virus infection in humans across 16 countries—April–June 2022. *New England Journal of Medicine* **2022**, *387*, 8, 679-691.
18. Khan, A.; Akram, M.; Thiruvengadam, M.; Daniyal, M.; Zakki, S.A.; Munir, N.; Zainab, R.; Heydari, M.; Mosavat, S.H.; Rebezov, M. Anti-anxiety properties of selected medicinal plants. *Current Pharmaceutical Biotechnology* **2022**, *23*, 1041-1060, https://doi.org/10.2174/1389201022666210122125131.
19. Hunter, N.; Rathish, B. Marburg Fever. In *StatPearls [Internet]*; StatPearls Publishing: **2022**, https://www.ncbi.nlm.nih.gov/books/NBK578176/.
20. Abir, M.H.; Rahman, T.; Das, A.; Etu, S.N.; Nafiz, I.H.; Rakib, A.; Mitra, S.; Emran, T.B.; Dhama, K.; Islam, A. Pathogenicity and virulence of Marburg virus. *Virulence* **2022**, *13*, 609-633, https://doi.org/10.1080%2F21505594.2022.2054760.

21. Lawrence, J.; Ul Rasool, M.; Parikh, C.; Chowdhury, S.; Sueldo, A. Emergence of Marburg Virus Disease in West Africa amid COVID-19 and Ebola: Efforts, Challenges, and Recommendations to Prevent the Next Public Health Crisis. *J Infect Dis Epidemiol* **2022**, *8*, 259, https://clinmedjournals.org/articles/jide/journal-of-infectious-diseases-and-epidemiology-jide-8-259.php?jid=jide.
22. Mahmud, S.N.; Rahman, M.; Kar, A.; Jahan, N.; Khan, A. Designing of an Epitope-Based Universal Peptide Vaccine against Highly Conserved Regions in RNA Dependent RNA Polymerase Protein of Human Marburg Virus: A Computational Assay. *Anti-Infective Agents* **2020**, *18*, 294-305, http://dx.doi.org/10.2174/2211352517666190717143949.
23. Hanieh, H.; Islam, V.I.H.; Saravanan, S.; Chellappandian, M.; Ragul, K.; Durga, A.; Venugopal, K.; Senthilkumar, V.; Senthilkumar, P.; Thirugnanasambantham, K.J.E.J.o.P. Pinocembrin, a novel histidine decarboxylase inhibitor with anti-allergic potential in in vitro. **2017**, *814*, 178-186, https://doi.org/10.1016/j.ejphar.2017.08.012.
24. Shen, X.; Liu, Y.; Luo, X.; Yang, Z.J.M. Advances in biosynthesis, pharmacology, and pharmacokinetics of pinocembrin, a promising natural small-molecule drug. **2019**, *24*, 2323, https://doi.org/10.3390/molecules24122323.
25. Wouters, O.J.; McKee, M.; Luyten, J. Estimated research and development investment needed to bring a new medicine to market, 2009-2018. *Jama* **2020**, *323*, 844-853, https://doi.org/10.1001/jama.2020.1166.
26. Lagunin, A.; Stepanchikova, A.; Filimonov, D.; Poroikov, V.J.B. PASS: prediction of activity spectra for biologically active substances. **2000**, *16*, 747-748, https://doi.org/10.1093/bioinformatics/16.8.747.
27. Parasuraman, S.J.J.o.p.; pharmacotherapeutics. Prediction of activity spectra for substances. **2011**, *2*, 52, https://doi.org/10.4103%2F0976-500X.77119.
28. Filimonov, D.; Lagunin, A.; Gloriozova, T.; Rudik, A.; Druzhilovskii, D.; Pogodin, P.; Poroikov, V.J.C.o.H.C. Prediction of the biological activity spectra of organic compounds using the PASS online web resource. **2014**, *50*, 444-457, https://link.springer.com/article/10.1007/s10593-014-1496-1.
29. Kawsar, S.; Kumer, A.; Munia, N.S.; Hosen, M.A.; Chakma, U.; Akash, S. Chemical descriptors, PASS, molecular docking, molecular dynamics and ADMET predictions of glucopyranoside derivatives as inhibitors to bacteria and fungi growth. *Organic Communications* **2022**, *15*, https://www.acgpubs.org/article/organic-communications/2022/2-april-june/chemical-descriptors-pass-molecular-docking-molecular-dynamics-and-admet-predictions-of-glucopyranoside-derivatives-as-an-inhibitor-of-bacteria-and-fungi.
30. Kobir, M.E.; Ahmed, A.; Roni, M.A.H.; Chakma, U.; Amin, M.R.; Chandro, A.; Kumer, A. Anti-lung cancer drug discovery approaches by polysaccharides: an in silico study, quantum calculation and molecular dynamics study. *Journal of Biomolecular Structure and Dynamics* **2022**, 1-17, https://doi.org/10.1080/07391102.2022.2110156.
31. Sarkar M. A. Kawsar , A.K., Nasrin S. Munia , Mohammed A. Hosen , Unesco Chakma and Shopnil Akash. Chemical descriptors, PASS, molecular docking, molecular dynamics and ADMET predictions of glucopyranoside derivatives as inhibitors to bacteria and fungi growth. *Organic-communications* **2022**, https://doi.org/10.25135/acg.oc.122.2203.2397.
32. Minasov, G., Shuvalova, L., Dubrovska, I., Flores, K., Grimshaw, S., Kwon, K., Anderson, W.F. 1.52 Angstrom Crystal Structure of A42R Profilin-like Protein from Monkeypox Virus Zaire-96-I-16. (https://www.rcsb.org/structure/4QWO). *Center for Structural Genomics of Infectious Diseases (CSGID)*, http://doi.org/10.2210/pdb4QWO/pdb.
33. Zhang, A.P.; Bornholdt, Z.A.; Abelson, D.M.; Saphire, E.O.J.J.o.v. Crystal structure of Marburg virus VP24. **2014**, *88*, 5859-5863, https://doi.org/10.1128%2FJVI.03565-13.
34. De Oliveira, D.B.; Gaudio, A.C. BuildQSAR: a new computer program for QSAR analysis. *Quantitative Structure-Activity Relationships: An International Journal Devoted to Fundamental and Practical Aspects of Electroanalysis* **2000**, *19*, 599-601, https://doi.org/10.1002/1521-3838(200012)19:6%3C599::AID-QSAR599%3E3.0.CO;2-B.
35. Rahman, M.M.; Biswas, S.; Islam, K.J.; Paul, A.S.; Mahato, S.K.; Ali, M.A.; Halim, M.A. Antiviral phytochemicals as potent inhibitors against NS3 protease of dengue virus. *Computers in Biology and Medicine* **2021**, *134*, 104492, https://doi.org/10.1016/j.compbiomed.2021.104492.
36. Siddikey, F.; Roni, M.; Kumer, A.; Chakma, U.; Matin, M. Computational investigation of Betalain derivatives as natural inhibitor against food borne bacteria. *Current Chemistry Letters* **2022**, *11*, 309-320, http://dx.doi.org/10.5267/j.ccl.2022.3.003.
37. Rasul, A.; Millimouno, F.M.; Ali Eltayb, W.; Ali, M.; Li, J.; Li, X.J.B.r.i. Pinocembrin: a novel natural compound with versatile pharmacological and biological activities. *Biomedical Research International* **2013**, *2013*, https://doi.org/10.1155/2013/379850.
38. Bouř, P.; Keiderling, T.A.J.T.J.o.c.p. Partial optimization of molecular geometry in normal coordinates and use as a tool for simulation of vibrational spectra. J. Chem. Phys. **2002**, *117*, 4126-4132, https://doi.org/10.1063/1.1498468.
39. Akash, S.; Kumer, A.; Rahman, M.; Emran, T.B.; Sharma, R.; Singla, R.K.; Alhumaydhi, F.A.; Khandaker, M.U.; Park, M.N.; Idris, A.M. Development of new bioactive molecules to treat breast and lung cancer with natural myricetin and its derivatives: A computational and SAR approach. *Frontiers in Cellular and Infection Microbiology* **2022**, 1400, https://doi.org/10.3389/fcimb.2022.952297.

40. Kumer, A.; Chakma, U.; Matin, M.M.; Akash, S.; Chando, A.; Howlader, D.J.O.C. The computational screening of inhibitor for black fungus and white fungus by D-glucofuranose derivatives using in silico and SAR study. *World Health Organization* **2021**, *14*, https://search.bvsalud.org/global-literature-on-novel-coronavirus-2019-ncov/resource/en/covidwho-1614497.
41. Rahman, M.M.; Islam, M.R.; Akash, S.; Mim, S.A.; Rahaman, M.S.; Emran, T.B.; Akkol, E.K.; Sharma, R.; Alhumaydhi, F.A.; Sweilam, S.H.; et al. In silico investigation and potential therapeutic approaches of natural products for COVID-19: Computer-aided drug design perspective. *Frontiers in Cellular and Infection Microbiology* **2022**, *12*, https://doi.org/10.3389/fcimb.2022.929430.
42. Kawsar, S.; Kumer, A. Computational investigation of methyl α-D-glucopyranoside derivatives as inhibitor against bacteria, fungi and COVID-19 (SARS-2). *Journal of the Chilean Chemical Society* **2021**, *66*, 5206-5214, https://www.scielo.cl/scielo.php?pid=S0717-97072021000205206&script=sci_abstract.
43. Kumer, A.; Chakma, U.; Rana, M.M.; Chandro, A.; Akash, S.; Elseehy, M.M.; Albogami, S.; El-Shehawi, A.M. Investigation of the New Inhibitors by Sulfadiazine and Modified Derivatives of α-D-glucopyranoside for White Spot Syndrome Virus Disease of Shrimp by In Silico: Quantum Calculations, Molecular Docking, ADMET and Molecular Dynamics Study. *Molecules* **2022**, *27*, 3694, https://doi.org/10.3390/molecules27123694.
44. Matin, M.M.; Nath, A.R.; Saad, O.; Bhuiyan, M.M.; Kadir, F.A.; Abd Hamid, S.B.; Alhadi, A.A.; Ali, M.E.; Yehye, W.A. Synthesis, PASS-predication and in vitro antimicrobial activity of benzyl 4-O-benzoyl-α-L-rhamnopyranoside derivatives. *International Journal of Molecular Sciences* **2016**, *17*, 1412, https://doi.org/10.3390/ijms17091412.
45. KUMER, A.; Sarker, M.N.; Sunanda, P. The theoretical investigation of HOMO, LUMO, thermophysical properties and QSAR study of some aromatic carboxylic acids using HyperChem programming. *International Journal of Chemistry and Technology* **2019**, *3*, 26-37, https://dergipark.org.tr/tr/download/article-file/702384.
46. Islam, M.J.; Kumer, A.; Paul, S.; Sarker, M. The activity of alkyl groups in morpholinium cation on chemical reactivity, and biological properties of morpholinium tetrafluroborate ionic liquid using the DFT method. *Chemical Methodologies* **2020**, *4*, 130-142, http://www.chemmethod.com/article_89953.html.
47. Kumer, A.; Sarker, M.N.; Sunanda, P. The simulating study of HOMO, LUMO, thermo physical and quantitative structure of activity relationship (QSAR) of some anticancer active ionic liquids. *Eurasian Journal of Environmental Research* **2019**, *3*, 1-10, https://dergipark.org.tr/en/pub/ejere/issue/45416/478362.
48. Rahman, M.A.; Chakma, U.; Kumer, A.; Rahman, M.R.; Matin, M.M. Uridine-Derived 4-Aminophenyl 1-Thioglucosides: DFT Optimized FMO, ADME, and Antiviral Activities Study. *Biointerface Research in Applied Chemistry* **2022**, http://dx.doi.org/10.33263/BRIAC131.052.
49. Sanaullah, A. F. M.; Devi, P.; Hossain, T.; Sultan, S. B.; Badhon, M. M. U.; Hossain, M.; et al. Rhamnopyranoside-Based Fatty Acid Esters as Antimicrobials: Synthesis, Spectral Characterization, PASS, Antimicrobial, and Molecular Docking Studies. *Molecules* **2023**, *28*, 986.
50. Cheng, F.; Li, W.; Liu, G.; Tang, Y.J.C.t.i.m.c. In silico ADMET prediction: recent advances, current challenges and future trends. **2013**, *13*, 1273-1289, https://doi.org/10.2174/15680266113139990033.
51. Rout, J.; Swain, B.C.; Tripathy, U.J.J.o.B.S.; Dynamics. In silico investigation of spice molecules as potent inhibitor of SARS-CoV-2. **2022**, *40*, 860-874, https://doi.org/10.1080/07391102.2020.1819879.
52. Pires, D.E.; Blundell, T.L.; Ascher, D.B. PkCSM: Predicting Small-Molecule Pharmacokinetic Properties Using Graph-Based Signatures. *J. Med. Chem.* **2015**, *58*, 4066-4072, https://doi.org/10.1021/acs.jmedchem.5b00104.
53. Akash, S. Computational screening of novel therapeutic and potent molecules from bioactive trehalose and it's eight derivatives by different insilico studies for the treatment of diabetes mellitus, https://www.acgpubs.org/article/organic-communications/2022/3-july-september/development-of-novel-therapeutic-and-potent-molecules-from-bioactive-trehalose-and-its-derivatives-by-insilico-and-sar-studies.
54. Kumer, A.; Chakma, U.; Chandro, A.; Howlader, D.; Akash, S.; Kobir, M.; et al. Modified D-glucofuranose computationally screening for inhibitor of breast cancer and triple breast cancer: Chemical descriptor, molecular docking, molecular dynamics and QSAR. *Journal of the Chilean Chemical Society*, **2022**, *67*, 5623-5635.
55. Gaulton, A.; Bellis, L.J.; Bento, A.P.; Chambers, J.; Davies, M.; Hersey, A.; Light, Y.; McGlinchey, S.; Michalovich, D.; Al-Lazikani, B.J.N.a.r. ChEMBL: a large-scale bioactivity database for drug discovery. **2012**, *40*, D1100-D1107, https://doi.org/10.1093/nar/gkr777.
56. Rahman, M.A.; Matin, M.M.; Kumer, A.; Chakma, U.; Rahman, M. Modified D-glucofuranoses as new black fungus protease inhibitors: Computational screening, docking, dynamics, and QSAR study. *Physical Chemistry Research* **2022**, *10*, 195-209, https://search.bvsalud.org/global-literature-on-novel-coronavirus-2019-ncov/resource/en/covidwho-1579475.
57. Nkungli, N. K.; Fouegue, A. D. T.; Tasheh, S. N.; Bine, F. K.; Hassan, A. U.; Ghogomu, J. N. In silico investigation of falcipain-2 inhibition by hybrid benzimidazole-thiosemicarbazone antiplasmodial agents: A molecular docking, molecular dynamics simulation, and kinetics study. *Molecular Diversity*, **2023**, 1-22.
58. Rahman, M.A.; Matin, M.M.; Kumer, A.; Chakma, U.; Rahman, M.J.P.C.R. Modified D-Glucofuranoses as New Black Fungus Protease Inhibitors: Computational Screening, Docking, Dynamics, and QSAR Study.

2022, *10*, 195-209, https://search.bvsalud.org/global-literature-on-novel-coronavirus-2019-ncov/resource/en/covidwho-1579475.

Supplementary materials

Table 1. *Protein*- ligands interaction with amino acid (AA) residues and their bond distance.

Amino acid (AA) residues with *Monkeypox Virus (PDB ID 4QWO)*

NO	Name	Distance	Category	Type
01	A: SER-12	3.14518	Hydrogen Bond	Conventional Hydrogen Bond
	A: HIS-5	2.0005	Hydrogen Bond	Conventional Hydrogen Bond
	A: GLU-9	2.95522	Hydrogen Bond	Conventional Hydrogen Bond
	A: ILE-35	3.7894	Hydrophobic	Pi-Sigma
	A: ILE-35	3.92387	Hydrophobic	Pi-Sigma
	A:PRO-36	4.84679	Hydrophobic	Pi-Alkyl
02	A: GLU-9	2.84233	Hydrogen Bond	Conventional Hydrogen Bond
	A: GLU-9	3.61449	Electrostatic	Pi-Anion
	A: SER-12	3.32335	Hydrogen Bond	Pi-Donor Hydrogen Bond
	A: ILE-35	3.51974	Hydrophobic	Pi-Sigma
	A: ILE-35	3.5692	Hydrophobic	Pi-Sigma
03	A: GLU-9	3.6961	Electrostatic	Pi-Anion
	A: SER-12	3.32724	Hydrogen Bond	Pi-Donor Hydrogen Bond
	A: ILE-35	3.55037	Hydrophobic	Pi-Sigma
	A: ILE-35	3.59213	Hydrophobic	Pi-Sigma
04	A:PRO-36	3.05619	Hydrogen Bond	Carbon Hydrogen Bond
	A: PHE-17	3.09242	Halogen	Halogen (Fluorine)
	A: GLU-18	2.973	Halogen	Halogen (Fluorine)
	A: GLU-9	4.81166	Electrostatic	Pi-Anion
	A: SER-12	3.88183	Hydrogen Bond	Pi-Donor Hydrogen Bond
	A: ILE-35	3.74746	Hydrophobic	Pi-Sigma
	A: ILE-35	3.8297	Hydrophobic	Pi-Sigma
05	A: GLU-9	3.6204	Electrostatic	Pi-Anion
	A: SER-12	3.35478	Hydrogen Bond	Pi-Donor Hydrogen Bond
	A: ILE-35	3.53577	Hydrophobic	Pi-Sigma
	A: ILE-35	3.57856	Hydrophobic	Pi-Sigma
06	A: GLU-9	3.5542	Electrostatic	Pi-Anion
	A: SER-12	3.35096	Hydrogen Bond	Pi-Donor Hydrogen Bond
	A: ILE-35	3.54662	Hydrophobic	Pi-Sigma
	A: ILE-35	3.58942	Hydrophobic	Pi-Sigma
07	A: GLU-9	3.65988	Electrostatic	Pi-Anion
	A: SER-12	3.35032	Hydrogen Bond	Pi-Donor Hydrogen Bond
	A: ILE-35	3.56046	Hydrophobic	Pi-Sigma
	A: ILE-35	3.60549	Hydrophobic	Pi-Sigma
08	A: GLU-9	3.70312	Electrostatic	Pi-Anion
	A: SER-12	3.33084	Hydrogen Bond	Pi-Donor Hydrogen Bond
	A: ILE-35	3.56	Hydrophobic	Pi-Sigma
	A: ILE-35	3.59948	Hydrophobic	Pi-Sigma

Amino acid (AA) residues with *Marburg virus (PDB 4OR8)*

NO	Name	Distance	Category	Type
01	B: THR-72	3.58745	Hydrogen Bond	Pi-Donor Hydrogen Bond
	B: VAL-193	3.92783	Hydrophobic	Pi-Sigma
	B: MET-195	4.9391	Other	Pi-Sulfur
	B: LEU-198	5.04295	Hydrophobic	Pi-Alkyl
	B: LEU-223	5.28125	Hydrophobic	Pi-Alkyl
02	B: VAL-193	3.9054	Hydrophobic	Pi-Sigma
	B: MET-195	4.99661	Other	Pi-Sulfur
	B: LEU-198	4.9602	Hydrophobic	Pi-Alkyl
	B: LEU-223	5.24999	Hydrophobic	Pi-Alkyl
03	B: THR-72	3.54858	Hydrogen Bond	Pi-Donor Hydrogen Bond
	B: VAL-193	3.93642	Hydrophobic	Pi-Sigma
	B: VAL-193	3.79452	Hydrophobic	Pi-Sigma
	B: MET-195	4.94436	Other	Pi-Sulfur
	NB: LEU-198	5.11156	Hydrophobic	Pi-Alkyl
	B: LEU-223	5.37298	Hydrophobic	Pi-Alkyl
04	B: THR-72	3.58883	Hydrogen Bond	Pi-Donor Hydrogen Bond
	B: VAL-193	3.90494	Hydrophobic	Pi-Sigma

	B: VAL-193 B: MET-195 B: LEU-198 B: LEU-223	3.79058 4.98521 5.10018 5.40516	Hydrophobic Other Hydrophobic Hydrophobic	Pi-Sigma Pi-Sulfur Pi-Alkyl Pi-Alkyl
05	B: VAL193 B: MET-195 B: LEU—198 B: LEU-223	3.92304 5.03596 4.97327 5.311	Hydrophobic Other Hydrophobic Hydrophobic	Pi-Sigma Pi-Sulfur Pi-Alkyl Pi-Alkyl
06	B: VAL-193 B: MET-195 B: LEU-198 B: LEU-223	3.9209 4.99252 4.96117 5.24513	Hydrophobic Other Hydrophobic Hydrophobic	Pi-Sigma Pi-Sulfur Pi-Alkyl Pi-Alkyl
07	B:ASP-172 B: ASN-171 B: VAL-193 B: MET-195 B: LEU-198 B: LEU-223	3.39445 3.41816 3.9116 5.03135 4.94716 5.27497	Hydrogen Bond Hydrogen Bond Hydrophobic Other Hydrophobic Hydrophobic	Conventional Hydrogen Bond Carbon Hydrogen Bond Pi-Sigma Pi-Sulfur Pi-Alkyl Pi-Alkyl
08	B: GLN-71 B: THR-72 B: LEU-75 B: LEU-75 B: VAL-170 B: VAL-193 B: MET-195 B: LEU-223	3.96784 3.56471 3.42374 3.73192 5.09608 4.75099 4.73267 5.12294	Hydrogen Bond Hydrogen Bond Hydrophobic Hydrophobic Hydrophobic Hydrophobic Hydrophobic Hydrophobic	Pi-Donor Hydrogen Bond Pi-Donor Hydrogen Bond Pi-Sigma Alkyl Pi-Alkyl Pi-Alkyl Pi-Alkyl Pi-Alkyl

[Note: TRP =Tryptophan, ASP = Aspartic acid, GLU = Glutamic acid, LEU = Leucine, THR = Threonine, ASN = Asparagine, GLN = Glutamine, PHE = Phenylalanine, ILE = Isoleucine, ARG = Arginine, VAL = Valine, SER = Serine, PRO = Proline, GLY = Glycine, HIS = Histidine, LYS = Lysine, TRP = Tryptophan, CYS = Cysteine, MET = Methionine.]